Korean Chem. Eng. Res., 62(1), 112-117 (2024)
https://doi.org/10.9713/kcer.2024.62.1.112
PISSN 0304-128X, EISSN 2233-9558

Numerical Simulation on the Onset of Radial Fingering in a Hele-Shaw Cell or a Porous Medium

Min Chan Kim†

Department of Chemical Engineering, Jeju National University, Jeju, 63243, Korea
(Received 3 December 2023; Received in revised from 26 December 2023; Accepted 27 December 2023)

Abstract – Numerical simulations on the onset and the growth of viscous fingering during the miscible displacement due to the radial source flow were conducted. With introduction of a new stability criterion, the critical log-viscosity ratio, R_c, was found as a function of the Peclet number, Pe. Similar to the previous linear stability analyses, Pe made the system unstable, *i.e.*, accelerated the onset of instability. For a large Pe system, the present numerical simulation yielded much stable results than the previous theoretical predictions This discrepancy was commonly encountered in the comparison between the theoretical prediction and the experimental finding. Additionally, the difference between the rectilinear system and the present one was also discussed. The present system was found more insensitive to the Peclet number than the rectilinear one.

Key words: Viscous fingering, Radial source flow, Stability analysis, Numerical simulation

1. Introduction

When more viscous fluid is displaced by a less viscous one, hydrodynamic instability known as viscous fingering (VF) can be induced due to the viscosity mismatch [1]. Since, viscous fingering phenomena play important roles in a wide variety of applications, such as enhanced oil recovery, fixed bed regeneration in chemical processing, hydrology, filtration, and so on, miscible VF has attracted many researcher's interests. Under the linear stability theory, Tan and Homsy derived stability equations in a radial Hele-Shaw cell or a porous medium and obtained the stability limits for the onset of radial viscous fingering in a porous medium [2]. Later, Pritchard studied double diffusive effects on the onset of radial viscous fingering [3]. By considering the double diffusive effects, he derived linear stability equations and described disturbance quantities based on an eigenfunction expansion method which enabled us to investigate the structure of the discrete eigenvalue spectrum. Inspired by Pritchard's approach, Kim revisited Tan and Homy's radial viscous fingering problem by suggesting eigenfunctions and corresponding eigenvalue spectrums [2-5].

Recently, using the Linear Stability Analysis (LSA) and Nonlinear Numerical Simulations (NNSs), Sharma et al. determined the critical conditions for the onset of viscous fingering as a function of log-viscosity ratio (R), the dimensionless radius of injection port (r_i), and Peclet number (Pe) [6]. Unlike Tan and Homy's normal mode analysis, Sharma et al. traced the amplification of the disturbance energy by treating the linearized stability equation as an initial value problem (IVP) [2,6]. In their LSA, they found that diffusive forces inhibited the growth of the disturbances and therefore, retarded the onset of instability motions. They also found that the relative intensity of the diffusive forces over the convective one can be controlled by the radius of the injection port, r_i. According to their linear and nonlinear numerical simulations, the larger the inlet diameter was, the more stable the system. Based on the results of the NNSs, Sharma et al. proposed the following critical log-viscosity ratio:

$$R_c = \alpha(r_i)Pe^{-\beta} \text{ with } 0.52 \le \beta \le 0.59$$

for the range of $r_i \in [0.1, 0.3]$ and $Pe \in [500, 10^4]$ [6]. Additionally, through the experiments, Sharma et al. showed that the instabilities were suppressed by increasing the radius of the injection port [6]. Later, Nand et al. experimentally analyzed the effects of the gap size of the Hele-Shaw cell on the stability characteristics of the radial VF [7]. Furthermore, they confirmed their experimental findings bythe 3-dimensional numerical simulations. As suggested by Kim, the onset of instability was hindered and the width of the fingers increased with an increment in the gap, which further weakened convective motion and therefore, decreased the Peclet number [4].

Since the analytic base fields were not known except for the limiting case of point source flow, *i.e.*, $r_i \to 0$, Sharma et al. and Nand et al., didn't try to compare their numerical simulations with Tan and Homy's and Kim's (2012) theoretical predictions obtained under the linear stability analysis [2,6-7]. In the present study, we tried to fill the gap between Tan and Homy's and Kim's theoretical stability analyses and Sharma et al.'s numerical simulations [2,4,6]. For the limiting case of point source flow, where analytical analysis was

† To whom correspondence should be addressed.
E-mail: mckim@jejunu.ac.kr

possible, the critical conditions for the onset of radial VF were numerically determined and compared with the previous theoretical predictions.

2. Base System and Governing Equations

Let us consider a two-dimensional Hele-Shaw cell (see Fig. 1) in which a solution in concentration C_0 was injected radially from a source at $r'=0$ with a constant areal flux Q (volume flow rate per unit depth) into a domain initially filled with a solution in concentration C_∞. If the viscosity of the displacing solution, μ_0, was lower than that of the displaced one, μ_∞, the flow system can be hydrodynamically unstable and induce the viscous fingering motion. The governing equations for the conservation of mass, the conservation of momentum in the form of Hele-Shaw approximation, and the convection-dispersion-reaction mass balance equation were given by,

$$\nabla\cdot\mathbf{U}=0\,, \tag{1}$$

$$\nabla P=-\frac{\mu}{K}\mathbf{U}\,, \tag{2}$$

$$\frac{\partial c}{\partial t}+\mathbf{U}\cdot\nabla C=D\nabla^2 C\,, \tag{3}$$

Here, $\mathbf{U}\{=(U,V,0)\}$ was the velocity vector, P the pressure, μ the viscosity, K the permeability, C the concentration of solute in a solution, and D the dispersion coefficient of a solute in a solvent [2,4,5]. Here, we assume that the fluid was incompressible and Newtonian. In addition, the injection condition can be derived as

$$2\pi r'\mathbf{U}\cdot\mathbf{n}=Q \text{ at } r'=R_i \tag{4}$$

where $\mathbf{n}$ was the outward normal unit vector and R_i was the diameter of the inlet port. Here, we ignored the non-linear drag effect which was considered by Kim [8].

In the cylindrical (r, θ)-coordinate, where $\mathbf{U}\{=(U_r,U_\theta,0)\}$, the dimensionless governing equations can be written as

$$\nabla\cdot\mathbf{u}=0\,, \tag{5}$$

$$\nabla p=-\bar{\mu}\mathbf{u}\,, \tag{6}$$

$$\frac{\partial c}{\partial \tau}+\mathbf{u}\cdot\nabla c=\frac{1}{Pe}\nabla^2 c\,, \tag{7}$$

Here, $\sqrt{K}, K/Q, Q/(2\pi\sqrt{K})$, $\mu_0, \mu_0 Q/(2\pi\sqrt{K})$ and $\Delta C(=C_0-C\infty)$ were used as length, time, velocity, viscosity, pressure, and concentration scales, respectively. In addition, Pe was the Péclet number defined as [3,9]

$$Pe=\frac{Q}{2\pi D}\,. \tag{8}$$

The Péclet number means the ratio of the convective transfer rate and dispersive one, and the Damköhler number represents the ratio of the reaction time scale with respect to the mass transfer time scale. It should be noted that Pe was mainly controlled by the mass flux Q, and the inlet condition (4) can be rewritten as

$$ru_r=1 \text{ at } r=r_i\,, \tag{9}$$

where $u_r=2\pi U_r\sqrt{K}/Q$ and $r_i=R_i/\sqrt{K}$. In addition, the boundary conditions for the concentration field were

$$c=1 \text{ at } r=r_i \text{ and } c=0 \text{ as } r\to\infty\,. \tag{10a\&b}$$

To complete the above model, the viscosity variation with the concentration was assumed to be

$$\bar{\mu}=\exp(R(1-c))\,, \tag{11}$$

where R was the log-viscosity ratio defined as

$$R=\ln\left(\frac{\mu_\infty}{\mu_0}\right)\,. \tag{12}$$

3. Numerical Simulations

We solved the governing equations (5)-(12) in the 2-dimensional x-y domain by employing a finite element solver, COMSOL Multiphysics, which has been used to study viscous and gravitational fingering problems [9-15]. By combining Eqs. (5) and (6), we derive the following Poisson equation:

$$\nabla\cdot\left(-\frac{1}{\bar{\mu}}\nabla p\right)=0\,, \tag{13}$$

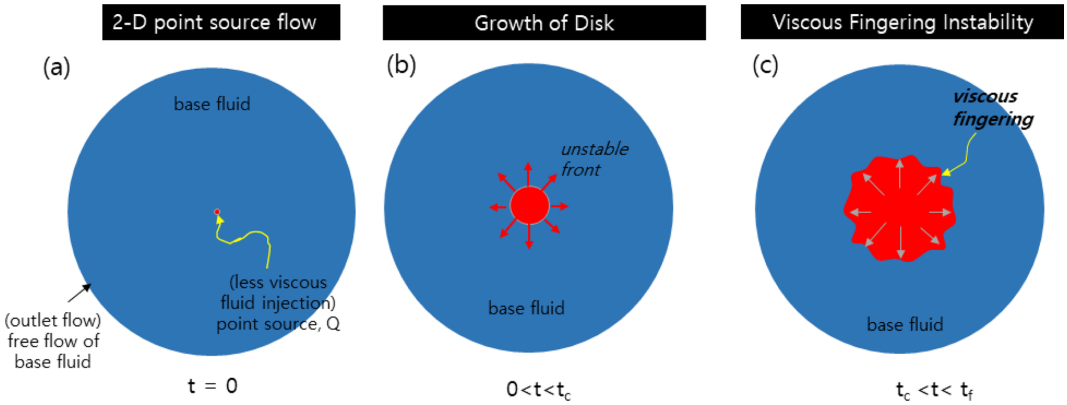

Fig. 1. Schematic diagram of system considered under investigation.

and solved it by using the Poisson equation solver (abbreviated as 'poeq' in the mathematics interface of COMSOL software). The inlet condition (9) was implemented as

$$\mathbf{u}\cdot\mathbf{n} = 1 \text{ at } r(=\sqrt{x^2+y^2}) = r_i . \tag{14}$$

For the point source system, *i.e.*, $r_i \to 0$, to treat the singular boundary condition (14), Verma et al. [16] approximated the velocity field as $\mathbf{u} = \mathbf{u}_{pot} + \mathbf{u}_{rot}$ and $p = p_{pot} + p_{rot}$, where

$$\mathbf{u} = \begin{cases} (x/(x^2+y^2), y/(x^2+y^2)) & \sqrt{x^2+y^2} > \sigma \\ (x/(x^2+y^2), y/(x^2+y^2))(1-\exp(-\sigma(x^2+y^2))) & \sqrt{x^2+y^2} \le \sigma \end{cases}, \tag{15}$$

$$\nabla\cdot\mathbf{u}_{rot} = 0 , \tag{16}$$

$$\nabla p_{rot} = -\mu\mathbf{u}_{rot} \tag{17}$$

However, in the present study, the point source condition, $ru_r \to 1$ as $r_i \to 0$ can be implemented by adding the following weak contribution at the injection point:

$$test(p)\overline{Q} \text{ at } x = y = 0 \tag{18}$$

where $\overline{Q}(= 2\pi r u_r) = 2\pi$ can be obtained using the inlet condition (9).

Unlike Tan and Homsy's and Kim's linear stability analysis, it was impossible to impose semi-infinite boundary conditions in the present numerical simulations [2,4]. Due to this limitation, we imposed the following outlet conditions at r_e (=1.5):

$$p = 1 \text{ and } \mathbf{n}\cdot\nabla c = 0 \text{ at } r(=\sqrt{x^2+y^2}) = r_e . \tag{19}$$

Then, by using Eq. (6), the velocity field was obtained and was used to solve the diffusion-advection equation (7). This diffusion-advection equation was solved by the stabilized convection-diffusion equation solver (abbreviated as 'scdeq' in the mathematics interface of COMSOL software using the following initial and boundary conditions [9]:

$$c = 0 \text{ at } \tau = 0 , \tag{20}$$

$$c = 1 \text{ at } r \le r_i \text{ and } c = 0 \text{ at } r = r_e . \tag{21a\&b}$$

Unlike the previous theoretical analyses, where semi-infinite time and space domains were assumed, in the present study we proceeded with numerical simulations for the ranges of $[0, \tau_f]$ and $[0, \tau_e]$. Here, we stress that unlike the previous studies, the present analysis was not dependent on the built-in modules of COMSOL software, *i.e.*, the present solution methods were in-house implementations of COMSOL software [10-16].

For the example case of Pe = 1000, τ_f = 1.5 and r_e = 2.5, the spatio-temporal evolution of the concentration fields for stable and unstable cases were compared in Fig. 2. Stable displacements were visible for $R = 0$ and $R = 0.5$, whereas VF motion in an unstable front was clearly shown for the case of $R = 1$. Furthermore, slightly unstable VF motion was visible around $R = 0.65$. To quantify the distortion of the concentration field by VF motion and the magnitude of instability motion, we traced the temporal evolution of the concentration field by defining the magnitudes of the velocity ($\|\mathbf{u}\|$) and concentration gradient (I), as

$$\|\mathbf{u}\| = \iint_\Omega \sqrt{u^2+v^2}\, d\Omega , \tag{22a}$$

$$\delta\|\mathbf{u}\| = \|\mathbf{u}(R,\tau)\| - \|\mathbf{u}(0,\tau)\| . \tag{22b}$$

$$I = \iint_\Omega \sqrt{\left(\frac{\partial c}{\partial x}\right)^2 + \left(\frac{\partial c}{\partial y}\right)^2}\, d\Omega , \tag{23a}$$

$$\delta I = \frac{|I(R,\tau) - I(0,\tau)|}{I(0,\tau)} . \tag{23b}$$

The quantity I, which was known as the interfacial length, has been widely used to quantify the enhancement of mixing due to convection [17]. Sharma et al. classified that the system was unstable if $\delta I(R,\tau_f) > 0$, otherwise stable [6]. However, as shown in Fig. 3, $\delta\|\mathbf{u}\| \approx 10^{-4}$ explained the present simulation results summarized in Fig. 2, *i.e.*, VF motion was visible around $R \approx 0.65$ for the case of τ_f = 1.5. Furthermore, there existed a critical time, τ_c, from which instability motion can be expected. From this point, we employed the following stability criteria:

$$R_c = \exists\min_R\{\ \tau, \delta\|\mathbf{u}\|((R, 0<\tau<\tau_f) \le \text{tol})\} \text{ with tol} = 10^{-4}, \tag{24a}$$

$$\tau_c = \min_\tau\{\exists\tau, \delta\|\mathbf{u}\|((R,\tau) \ge \text{tol})\} \text{ with tol} = 10^{-4}. \tag{24b}$$

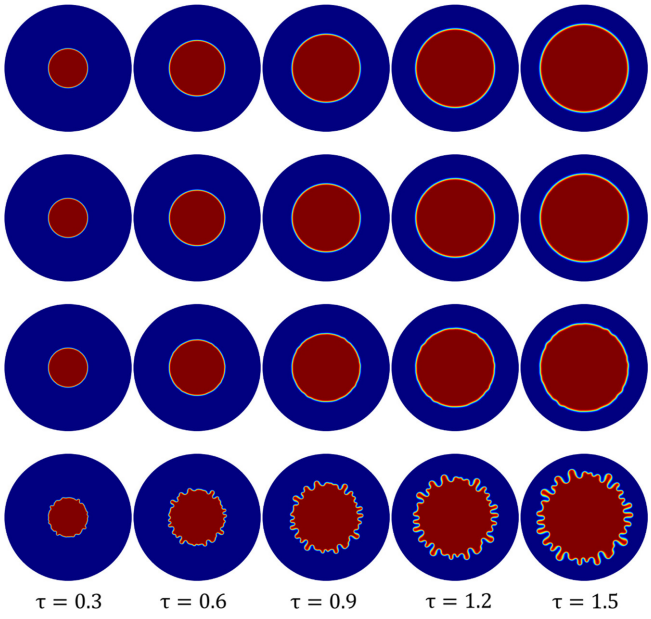

Fig. 2. Spatio-temporal evolution of concentration fields for Pe = 10^3, $R = 0$ (first raw), $R = 0.5$ (second raw), $R = 0.65$ (third raw), and $R = 1$ (fourth raw).

4. Results and Discussion

Sharma et al. [6] nondimensionalized the governing equations (2) by using the injection time, t_f, and $\sqrt{Qt_f}$ as the time and length scales. So, their Pe was different from the present one. Major differences between Sharma et al.'s and the present dimensionless parameters

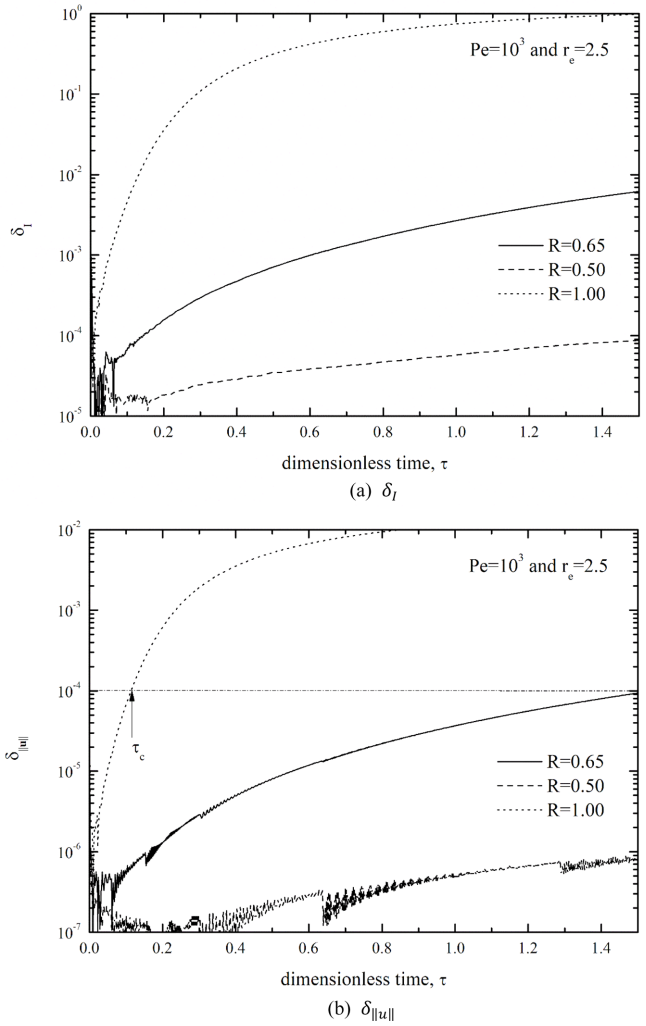

Fig. 3. Temporal evolution of (a) δ_I and $\delta_{\|u\|}$ (b) for the case of Pe = 10^3 and r_e = 2.5.

Table 1. Comparison of definitions and parameters used in the present study and the previous one

	Present study	Sharma et al. [6]
Radial velocity	$ru_r = 1$	$ru_r = \frac{1}{2\pi}$
Peclet no.	$\frac{Q}{2\pi D_A}$	$\frac{Q}{D_A}$
Dimensionless flux, $\overline{Q}$	2π	1

were summarized in Table 1 [6]. Numerically, Sharma et al.'s Pe_S and dimensionless time, τ_S, have the following relations with the present ones:

$$Pe_S = 2\pi Pe, \text{ and } \tau_S = 2\pi\tau, \quad (25a\&b)$$

Furthermore, it should be kept in mind that even though the Peclet number defined by Tan and Homsy was the same as Verma et al.'s, to keep Tan and Homsy's velocity field, $ru_r = 1$, their Pe should be rescaled by the present one [2,18]. Here, because we wanted to compare the previous theoretical predictions with FEM numerical

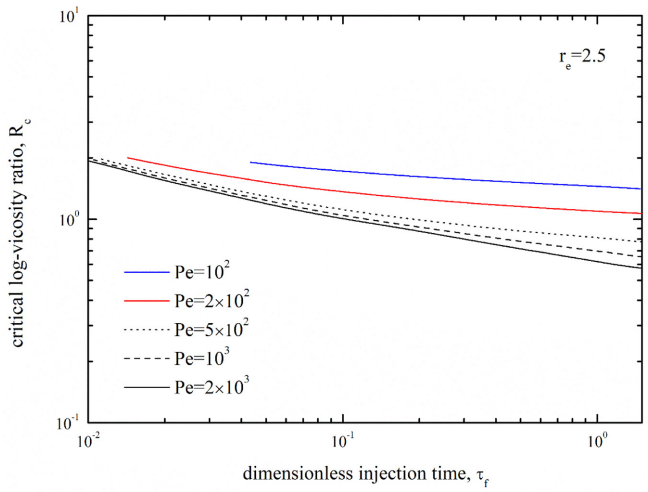

Fig. 4. Effect of injection time, τ_f, on the critical log-viscosity ratio, R_c.

simulations, we followed Tan and Homsy's scaling relations with modification.

Unlike the linear stability analyses where the critical conditions were determined in semi-infinite space and time domains, we cannot perform numerical simulation for unbounded domains. For some Pe cases, the effect of injection time, τ_f, on the critical log-viscosity ratio, R_c was summarized in Fig. 4. Since $\delta\|\mathbf{u}\|$ increased with time as discussed in Fig. 3, R_c decreased continuously with increasing τ_f. However, the decreasing rate, $dR_c/d\tau_f$, became smaller with increasing τ_f and decreasing Pe. Based on the above findings, we should choose a longer τ_f to minimize the discrepancy between the previous linear stability analyses and the present numerical simulations.

In the case of τ_f = 1.5 and r_f = 2.5, the critical log-viscosity ratio, R_c, was summarized in Fig. 5. For their time and length scales, Sharma et al. proposed the following relation [6]:

$$R = 30Pe_S^{-0.55} \text{ for } 500 < Pe_S < 10^4 \text{ and } \tau_S = 1, \quad (26a)$$

which was equivalent with

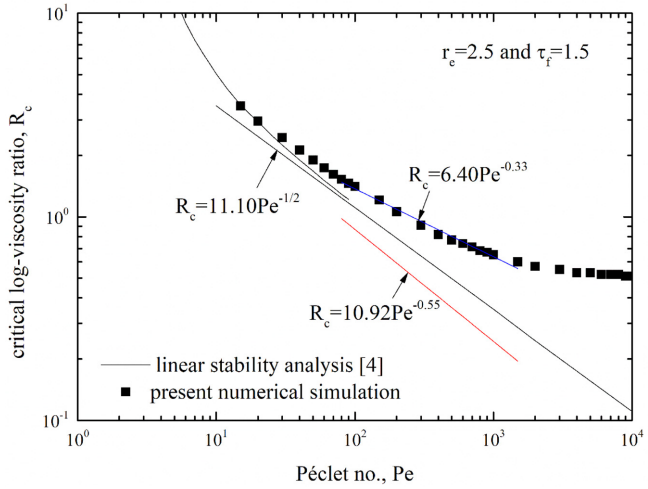

Fig. 5. Comparison of the present critical condition with previous theoretical and numerical studies.

$$R_c = 10.92\mathrm{Pe}^{-0.55} \quad \text{for } 80 < \mathrm{Pe} < 1600 \text{ and } \tau = 1/2\pi. \tag{26b}$$

However, their critical condition was far below the present one: $R_c = 10.92\mathrm{Pe}^{-0.55}$ for $80 < \mathrm{Pe} < 1600$. As shown in Fig. 5, their critical condition was far below the lower limit suggested by the linear stability analysis, their stability criterion, based on the interfacial length I may not be suitable for the present system. It should be kept in mind that the critical condition, R_c, was strongly dependent on the stability criterion and calculation domains. As shown in Figs. 3 and 4, if we extend our simulations for a longer time, *i.e.*, $\tau_f > 1.5$, R_c can be further lowered until the lower limit suggested by the linear stability analysis.

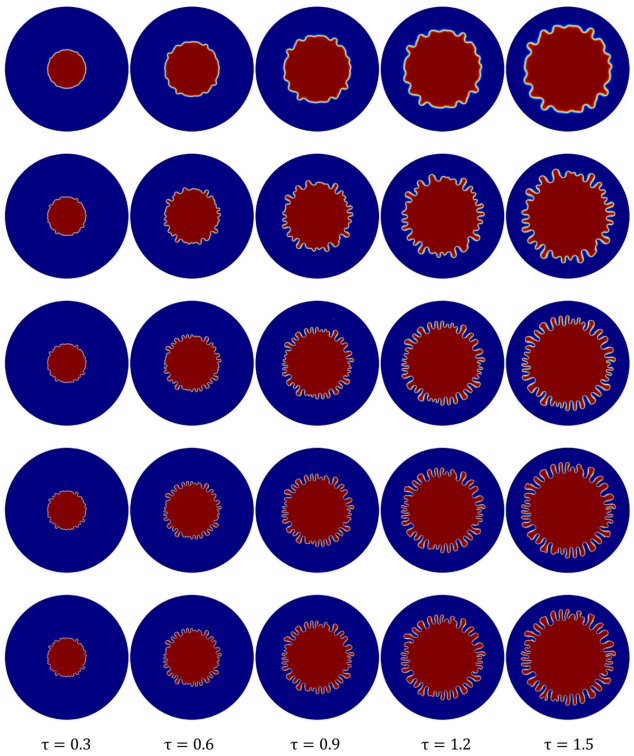

(a) spatio-temporal evolution of concentration fields for $R = 1$. $Pe = 500$ (first raw), $Pe = 10^3$ (second raw), $Pe = 2 \times 10^3$ (third raw), $Pe = 5 \times 10^3$ (fourth raw) and $Pe = 10^4$ (fifth raw)

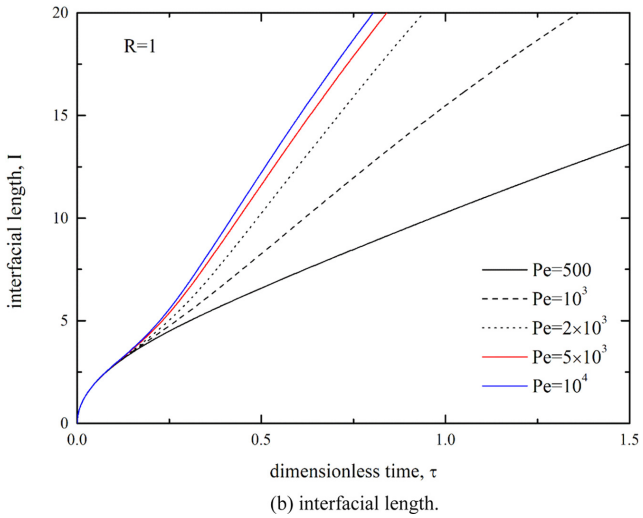

(b) interfacial length.

Fig. 6. Effects of the Peclet number on (a) the spatio-temporal evolution of concentration fields for $R = 1$ and (b) interfacial length.

As discussed in Figs. 3(b) and 4, there existed a critical time if the value of $R > R_c$. For the example case of $\mathrm{Pe} = 10^3$, the effect of the log-viscosity ratio on the critical time was summarized in Fig. 5. For the rectilinear system, based on the linear stability analysis, Ryoo and Kim and Kim and Pramanik suggested the following onset time [13,19]:

$$\tau_c \mathrm{Pe} = \alpha R^{-\beta}. \tag{27}$$

According to their analytic solution, for the limiting case of $R \ll 1$,

$$\alpha = 31.877 \text{ and } \beta = 2. \tag{28}$$

The above onset time was in good agreement the findings of Perkin's et al. [20] In addition, they proposed that the exponent β decreases with increasing R. However, less intention was given to the present radial VF system. The radial VF instability cannot be expected in the lower left region of each curve. Unlike the rectilinear system, regardless of R, τ_c, was relative insensitive to Pe, if $\mathrm{Pe} > 10^3$ [19]. It should be noted that the present τ_c and Pe_c were different from those for the previous continuous injection system because our simulations were conducted in finite space and time domains [2].

For a given fluids pair, the Péclect number can be controlled by the injection flow rate, Q. For the case of $R = 1$, the effect of Pe on the concentration field was summarized in Fig. 6. As shown in this figure, for the high Pe case, *i.e.*, $\mathrm{Pe} > 10^3$, Pe played little role in the temporal evolution of the concentration field. According to experiments of Sharma et al., even though the number of fingers increased with the volumetric injection rate, the average finger length was relatively insensitive to the injection rate.

5. Conclusions

The onset and the growth of the viscous fingering instability in a finite radial Hele-Shaw cell or a porous medium were analyzed numerically. Unlike the previous theoretical linear stability analysis, we studied the effects of the log-viscosity and Peclet number on the stability characteristics for the finite domain of $0 < \tau \le 1.5$ and $0 < r \le 2.5$. For a small Peclet number system, the current numerical simulations recovered the previous theoretical prediction whose domain corresponded to the semi-infinite domain of $0 < \tau \le \infty$ and $0 < r \le \infty$. However, for a highly large Peclet number system, the present simulations yielded more stable results than the linear stability analysis [8]. This discrepancy between the previous theoretical predictions and the present numerical simulation came from the difference in the calculation domain. The current simulations in the finite space and time domains show that the characteristics of radial VF were relatively insensitive to the Peclet number if $\mathrm{Pe} > 10^3$.

References

1. Homsy, G. M., "Viscous Fingering in Porous Medium," *Ann. Rev. Fluid Mech.* **19**, 271(1987).
2. Tan, C. T. and Homsy, G. M., "Stability of Miscible Displacements in Porous Media: Radial Source Flow," *Phys. Fluids* **30**, 1239(1987).
3. Pritchard, D., "The instability of Thermal and fluid Fronts During Radial Injection in a Porous Medium," *J. Fluid Mech.* **508**, 133 (2004)
4. Kim, M. C., "Onset of the Radial Viscous Fingering in a Hele-Shaw Cell," *Korean J. Chem. Eng.* **29**, 1688(2012).
5. Kim, M. C., "Some Analytical Aspects of the Radial Fingering in Porous Medium," *Z. Angew. Math. Phys.* **63**, 713(2012).
6. Sharma, V., Nand, S., Pramanik, S., Chen, C.-Y. and Mishra, M., "Control of Radial Viscous Fingering," *J. Fluid Mech.* **862**, 624 (2020).
7. Nand, S., Sharma, V., Das, S. K., Padhee, S. S. and Mishra, M., "Effect of Hele-Shaw Cell Gap on Radial Viscous Fingering," *Scientific Reports* **12**, 18967(2022).
8. Kim, M. C., "Effect of Nonlinear Drag on the Onset and the Growth of the Miscible Viscous Fingering in a Porous Medium," *Korean J. Chem. Eng.* **39**, 548(2022).
9. COMSOL AB, Comsol multiphysics v. 5.4 reference manual (2019).
10. Kim, M. C., Pramanik, S., Sharma, V. and Mishra, M., "Unstable Miscible Displacements in Radial flow with Chemical Reactions," *J. Fluid Mech.* **917**, A25(2021).
11. Sharma, V., Othman, H. B., Nagatsu, Y. and Mishra, M. "Viscous Fingering of Miscible Annular Ring," *J. Fluid Mech.* **916**, A14 (2021).
12. Kim, M. C., "Theoretical and Numerical Studies on the Interface Movement and the Onset of Gravitational Instability During the Carbon Dioxide Dissolution Into Oil," *Phys. Fluids* **34**, 024102 (2022).
13. Kim, M. C. and Pramanik, S., "Miscible Viscous Fingering in a Packed Cylindrical Column: Theory and Numerics," *Phys. Rev. Fluids* **8**, 013901(2023).
14. Hong, J. S. and Kim, M. C., "Theoretical and Numerical Studies on Dissolution of Horizontal Salt Body and Pattern Formation Incorporated with a Dynamic Moving Interface," *J. Fluid Mech.* **960**, A6(2023).
15. Hong, J. S. and Kim, M. C., "Gravitational Fingering and Droplet Formation During the Phase Separation of a Partially Miscible Binary Mixture in a Vertical Hele-Shaw Cell," *Int. J. Heat Mass Transfer* **201**, 123665(2023).
16. Kim, M. C., "Numerical Simulations on Thermocapillary Flow on Heated Sinusoidal Topography," *Korean J. Chem. Eng*. (2024). https://doi.org/10.1007/s11814-024-00109-1
17. Jha, B., Cueto-Felgueroso, L. and Juanes, R., "Fluid Mixing from Viscous Fingering," *Phys. Rev. Lett.* **106**, 194502(2011).
18. Verma, P., Sharma, V. and Mishra, M., "Radial Viscous Fingering Induced by An Infinitely Fast Chemical Reaction," *J. Fluid Mech.* **945**, A19(2022).
19. Ryoo, W. S. and Kim, M. C., "Linear and Non-linear Analyses on the Onset of Miscible Viscous Fingering in a Porous Medium," *Korean J. Chem. Eng.* **35**, 1423(2018).
20. Perkins, T. E., Johnston, O. E. and Hoffman, R. N., "Mechanics of Viscous Fingering in Miscible Systems," *Soc. Pet. Eng. J.*, **5**, 301(1965).

Authors

Min Chan Kim: Professor, Department of Chemical Engineering, Jeju National University, Jeju 63243, Korea; mckim@jejunu.ac.kr